ORGANOMETALLICS

Article

Cite This: Organometallics 2019, 38, 3961−3969

pubs.acs.org/Organometallics

Phosphine Oxide Based Supramolecular Ligands in the Rhodium-Catalyzed Asymmetric Hydrogenation

Julien Daubignard, Remko J. Detz, Bas de Bruin, and Joost N. H. Reek*

Van 't Hoff Institute for Molecular Sciences, University of Amsterdam, Science Park 904, Amsterdam 1098 XH, The Netherlands

Supporting Information

ABSTRACT: A series of bisphosphine monoxides and a phosphoramidite have been used for the preparation of supramolecular ligands. A structural analysis of the complexes using NMR spectroscopy and DFT calculations revealed the formation of strong hydrogen bonding between the two ligands. The complexes have been evaluated in the hydrogenation of several functionalized alkenes, leading to very high enantioselectivity for the substrates bearing a hydroxyl group. Also, kinetic studies showed that enhanced reaction rates of hydrogenation are observed in comparison with the supramolecular catalytic systems based on urea groups. In-depth NMR spectroscopy experiments and computational studies have highlighted the crucial role of the hydrogen bond between the phosphine oxide ligands and the substrate during the hydrogenation reaction.

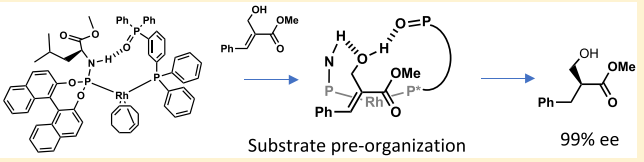

INTRODUCTION

The design of new catalysts is very important in the industry, especially in the field of fine chemicals and pharmaceuticals, in which time and cost are very important parameters in the development of new drugs.[1−3] Therefore, many ways to find new catalysts have been developed during the last decades. The high-throughput screening of known bidentate ligands that form the catalysts is a commonly applied strategy in the industry.[4−11] However, the sometimes difficult synthesis of highly asymmetric catalysts has required the use of new methods for the development of wide libraries of ligands. The versatility of monodentate ligands and their high efficiency in many reactions has quickly lifted them to the rank of privileged ligands.[12] Another approach developed by Reetz[13−17] and Feringa and de Vries[18−20] is the use of mixtures of monodentate ligands in the combinatorial screening of catalysts, expanding considerably the potential of monodentate ligands by increasing the number of possible catalysts that can be evaluated on the basis of a certain number of ligands. In another approach, several groups have reported the use of monodentate ligands that act as building blocks able to self-assemble through noncovalent interactions, leading to the formation of supramolecular catalysts.[21] Various interactions can be used for the assembly of ligand building blocks such as hydrogen bonds,[22−28] electrostatic interactions,[29−31] and metal−ligand association.[32−37] The search for catalysts based on new supramolecular systems is a developing field of research, and many concepts have to be explored.

We recently discovered a new series of supramolecular catalysts based on ligands that form supramolecular complexes through hydrogen bonding between the PNH group of a phosphoramidite and the carbonyl group of a urea-functionalized phosphine.[38] An extensive experimental mechanistic study demonstrated that intramolecular noncovalent interactions influence the reaction by the formation of a hydrogen bond between the catalyst and the substrate. Such interactions have been identified as decisive in the stereodiscriminating step of the reaction, and they also influence the rate.[39] Guided by rational design based on mechanistic considerations and computational studies, we have sought an improved catalyst that would enhance these supramolecular interactions.

Bisphosphine monoxides (BPMOs) are a class of ligands constituted of a phosphine group and a phosphine oxide group separated by a spacer (Figure 1). Due to the presence of both a hard (O) and soft (P) donor atom in the same structure, BPMOs constitute an important class of hemilabile ligands that can form labile metal chelates.[40]

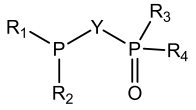

R_1, R_2, R_3, R_4 = alkyl, aryl...
Y= spacer

Figure 1. General structure of the bisphosphine monoxide ligands.

While BPMOs have been efficiently applied to several processes such as the carbonylation of methanol[41] and ethylene polymerization,[42] to the best of our knowledge, this class of ligand has never been investigated in the formation of

Special Issue: Asymmetric Synthesis Enabled by Organometallic Complexes

Received: July 18, 2019
Published: August 28, 2019

DOI: 10.1021/acs.organomet.9b00484
Organometallics 2019, 38, 3961−3969

supramolecular bidentate ligands. In this paper, we report a new class of supramolecular rhodium catalysts based on phosphine oxides as hydrogen bond acceptors combined with a chiral phosphoramidite to form bidentate supramolecular ligands. These complexes have been evaluated in the asymmetric hydrogenation of several benchmark substrates. While poor to moderate selectivities have been obtained for most of the substrates, excellent selectivity was observed in the hydrogenation of functionalized substrates bearing a hydroxyl group acting as a hydrogen bond directing group. More importantly, kinetic analysis revealed that this second generation of catalysts has higher hydrogenation rates in comparison to the urea-based system, while very high selectivity is maintained. Finally, by analysis of the contribution of the phosphine oxide group in the transition state during the reaction mechanism, these studies have led to a better understanding of this new class of supramolecular catalysts.

RESULTS AND DISCUSSION

We previously investigated the activity and the selectivity of the supramolecular complex [Rh(**1**)(**6**)]BF_4 (Figure 2) in the asymmetric hydrogenation of functionalized alkenes. Through an extensive mechanistic study, we have highlighted the crucial role of hydrogen bonding in the catalytic hydrogenation of a series of hydroxyl-functionalized substrates. As a result, the hydrogen bond acceptor (HBA) group of the urea-functionalized phosphine ligand has been identified as being actively involved at several stages of the catalytic cycle. First, this group is involved in the stabilization of the catalyst−substrate complex by forming hydrogen bonds with the substrate, enhancing the stereodiscrimination of the prochiral faces of the functionalized alkene. Also, computational studies showed that the same group is involved in the rate-determining step of the reaction (hydride migration step). Therefore, we anticipated that the modification of this group for a stronger hydrogen bond acceptor group would lead to possible beneficial changes in terms of enantioselectivity and activity.

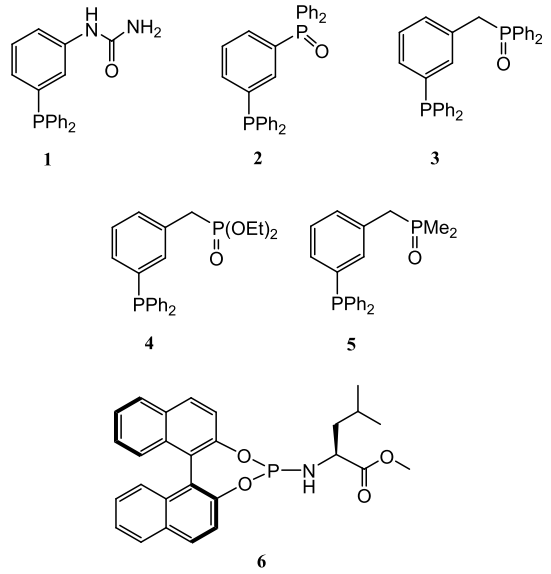

Figure 2. Structures of the bisphosphine monoxide ligands (**2**−**5**) and structure of the phosphoramidite ligand **6**.

As phosphine oxides are known to display strong HBA properties,[43−47] we decided to synthesize and evaluate a library of new BPMOs as HBAs in the formation of supramolecular bidentate ligands in rhodium complexes. On the basis of geometrical considerations and molecular modeling, ligands **3**−**5** were synthesized (Figure 2). The ligands were prepared in two steps in a fashion similar to that for the reported ligand UREAPhos (ligand **1**, Figure 2). The first step of the synthesis is the preparation of iodobenzyl derivatives by deprotonation of the corresponding phosphine oxide and the nucleophile addition on 3-iodobenzyl bromide. In a second step, the iodobenzyl derivatives are coupled with diphenylphoshine to give ligands **3**−**5** (Scheme 1).[48]

Scheme 1. Synthesis of the Ligands 3−5

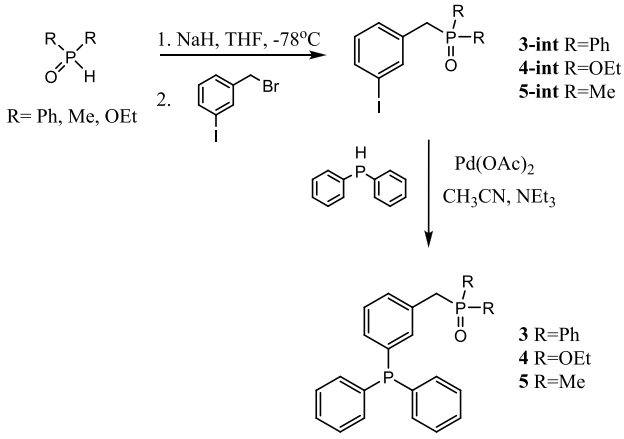

Ligands **2**−**5** were evaluated in the formation of supramolecular complexes in combination with phosphoramidite **6** (Figure 2). Mixing 1 equiv of ligand **3** with 1 equiv of phosphoramidite **6** and 1 equiv of [Rh(cod)$_2$]BF_4 (with cod = 1,5-cyclooctadiene) in CD_2Cl_2 results in the observation of a single species, as evidenced by ^{31}P NMR spectroscopy.

As can be seen in Figure 3, the ^{31}P NMR spectrum displays classic patterns for a heterocomplex (rhodium bearing two different ligands) with two doublets of doublets attributed to the phosphoramidite and the phosphine ligands and a sharp singlet attributed to the phosphine oxide moiety ($\delta(P^1)$ dd, 131.9 ppm, $^1J_{P,Rh}$ = 240.8 Hz, $^2J_{P,P'}$ = 31.3 Hz; $\delta(P^2)$ dd, 34.7 ppm, $^1J_{P,Rh}$ = 150 Hz, $^2J_{P,P'}$ = 31.3 Hz, $\delta(P^3)$ s, 32.4 ppm). In the ^{31}P NMR spectrum, a difference in chemical shift was observed for the PO moiety in comparison to the free ligand ($\Delta\delta$ = 4.1 ppm downfield shift). The relatively small change in

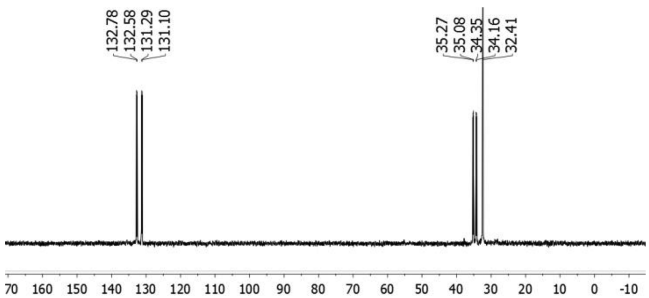

Figure 3. ^{31}P NMR spectrum of the complex [Rh(**3**)(**6**)(cod)]BF_4 in CD_2Cl_2 (162 MHz).

DOI: 10.1021/acs.organomet.9b00484
Organometallics 2019, 38, 3961−3969

chemical shift suggests that the phosphine oxide is not coordinated to the metal center, since much larger chemical shifts are usually observed in chelating BPMO-rhodium complexes.[49] Since no shift of the phosphine oxide moiety is expected upon coordination of the phosphine ligand,[40] the difference in chemical shift implies the involvement of the PO moiety in a hydrogen bond. We previously demonstrated by NMR experiments combined with X-ray crystallography that the ^{1}H chemical shift of the NH group of the phosphoramidite can be used as an indicator for the formation of hydrogen bonding between two ligands.[39] Therefore, we also performed a 2D $^{1}H-^{1}H$ COSY NMR experiment on the complex [Rh(**3**)(**6**)(cod)]BF_4 in CD_2Cl_2 in order to identify the signal of the PNH group of the phosphoramidite (δ_H 7.18 ppm). This large downfield chemical shift clearly indicates the formation of a hydrogen bond between the two ligands.[50] In a similar way, the quantitative formation of heterocomplexes was also observed for the complexes [Rh(**2**)(**6**)(cod)]BF_4, [Rh(**4**)(**6**)(cod)]BF_4, and [Rh(**5**)(**6**)(cod)]BF_4. The chemical shifts of the PNH groups in the different complexes as well as the chemical shifts of the PO groups are reported in Table 1.

Table 1. Chemical Shift of the PNH Group of the Complexes [Rh(L)(6)(cod)]BF_4 and the Corresponding Chemical Shift of the PO Group[a]

ligand	δ_{NH} (ppm)	$\Delta\delta_{NH}$	$\Delta\delta_{PO}$
PPh_3	4.25		
2	4.88	0.63	0.11
3	7.18	2.93	4.11
4	6.05	1.80	1.18
5	7.07	2.82	2.28

[a] $\Delta\delta(PO) = \delta(PO_{complex}) - \delta(PO_{free\ ligand})$.

Interestingly, the differences in the chemical shift of the PNH goups (with and without H bonds) are correlated with the difference in chemical shift of the corresponding PO group, suggesting a difference in the strength of the hydrogen bonds in the formation of supramolecular complexes.

From Table 1, a large difference in $\Delta\delta$(NH), and thus in the hydrogen bond strength, is observed between the complexes [Rh(**2**)(**6**)(cod)]BF_4 and [Rh(**3**)(**6**)(cod)]BF_4. In these two ligands, the substituents on the phosphine oxide moieties are phenyl groups. However, the introduction of the methylene spacer in [Rh(**3**)(**6**)(cod)]BF_4 induces an important variation in the geometry of the ligand. As a consequence, the geometry of the ligand influences the directionality of the HBA in the supramolecular complex and therefore leads to a significant change in the hydrogen bond strength.[51] Interestingly, the similar change in chemical shift observed for the NH in complexes [Rh(**3**)(**6**)(cod)]BF_4 and [Rh(**5**)(**6**)(cod)]BF_4 suggests that the electronic properties and the bulk of the phosphine oxide substituents do not significantly influence the strength of the hydrogen bond between the two ligands.

The stability of the supramolecular complexes [Rh(**2**)(**6**)(cod)]BF_4, [Rh(**3**)(**6**)(cod)]BF_4, [Rh(**4**)(**6**)(cod)]BF_4, and [Rh(**5**)(**6**)(cod)]BF_4 have been studied by means of DFT calculations in an examination of geometries in which a hydrogen bond exists between the two ligands, and these were compared to analogues in which this was absent. These structures were optimized, and the free energies of the corresponding supramolecular complexes were compared (Figures 4 and 5). For each complex, the conformers

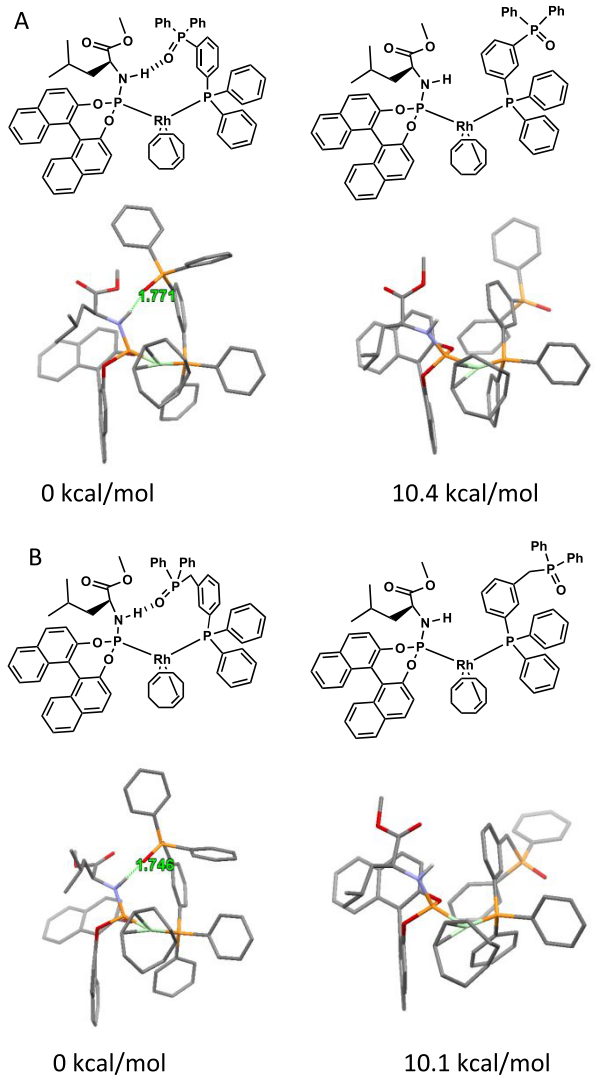

Figure 4. DFT optimized structures of the two conformers (with and without hydrogen bonding) of the different supramolecular complexes: (a) Rh(**2**)(**6**)(cod); (b) Rh(**3**)(**6**)(cod), The H-bond length, in green, is given in angstroms.[52]

displaying a hydrogen bond between the two ligands were found to be more stable than the corresponding conformers without a hydrogen bond. Also, the length of the hydrogen bond was measured and used as an indication of the strength. It shows that the hydrogen bond in complex [Rh(**2**)(**6**)(cod)]BF_4 is weaker than those in the other complexes, in line with the NMR experiments.

The complexes were evaluated in the asymmetric hydrogenation of several benchmark substrates (substrates **A**–**G**, Figure 6) and compared to the results obtained with the first generation of catalysts of this type (complex [Rh(**1**)(**6**)(cod)]BF_4). Since a variation of the hydrogen pressure can influence the selectivity of the catalytic reaction, we evaluated the performance of the complexes in the range 5–40 bar.[53]

As can be seen from Table 2, all of the catalysts give a similar trend in the selectivity in the hydrogenation of the substrates **A**–**E** (low selectivity for substrates **A**–**C** and **E** while good selectivity is obtained for substrate **D**) with up to 93% ee in the hydrogenation of substrate **D** by complex [Rh(**4**)(**6**)(cod)]BF_4 at 10 bar of H_2. Notably, substrate **D** is the only substrate next to **F** and **G** to have the same ester moiety and no amide,

DOI: 10.1021/acs.organomet.9b00484
Organometallics 2019, 38, 3961–3969

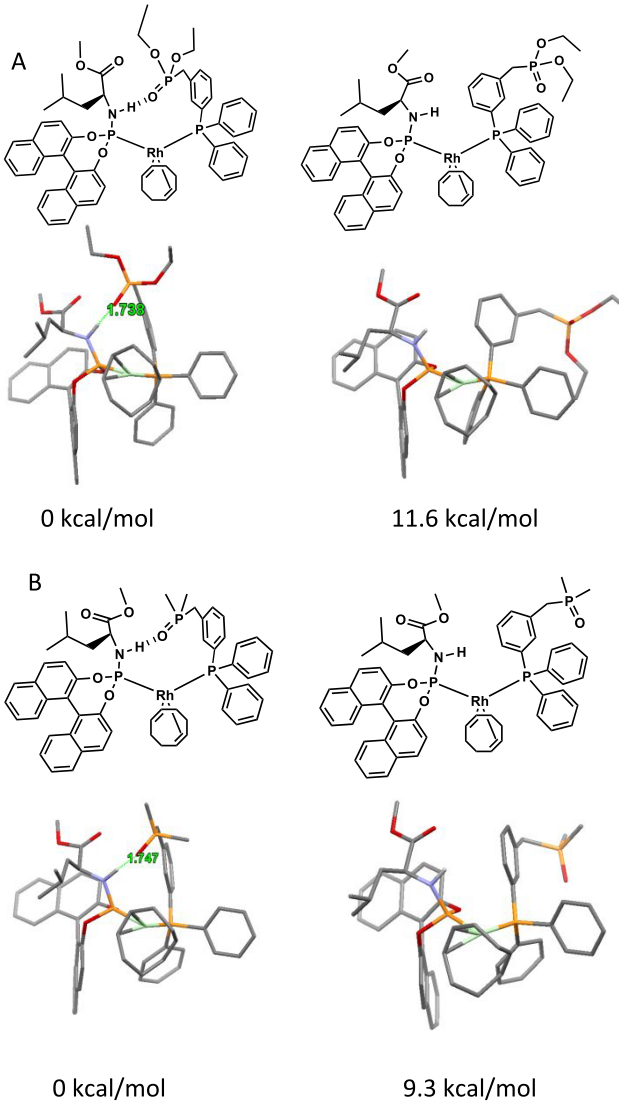

Figure 5. DFT optimized structures of the two conformers (with and without hydrogen bonding) of the different supramolecular complexes: (a) Rh(**4**)(**6**)(cod); (b) Rh(**5**)(**6**)(cod). The H-bond length, in green, is given in angstroms.[52]

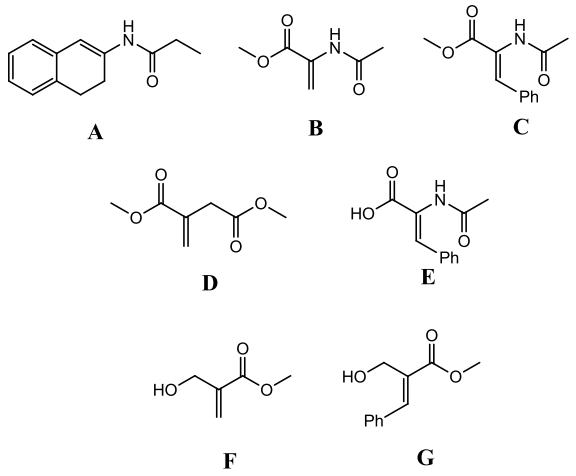

Figure 6. Substrates evaluated in the asymmetric hydrogenation reaction.

Table 2. Enantiomeric Excess (%) Obtained in the Hydrogenation of Substrates A–G by Complexes [Rh(L)(6)(cod)]BF_4[a]

	L				
substrate	1	2	3	4	5
A	16	30	0	0	7
B	12	22	14	38	34
C	34	41	30	36	44
D	92	88	92	93	87
E	0	8	18	23	19
F	99	96	99	99	99
G[b]	99	91	99	99	99

[a]Reagents and conditions unless noted otherwise: [Rh] = 0.2 mM, [substrate] = 0.1 M, CH_2Cl_2, 10 bar H_2, room temperature, 16 h. Conversions were determined by ^{1}H NMR or GC analysis. Full conversions were obtained for all the tested substrates except for substrate **A** (conversions ranging from 20 to 50%). The ee values were determined by chiral GC or HPLC analysis. [b][Rh] = 1 mM.

suggesting that the chelate complex that is formed with rhodium is similar. Also, the selectivity is rather independent of the pressure of hydrogen (see the Supporting Information). Substrates **F** and **G** (the substrates bearing a hydroxyl group) are hydrogenated with very high selectivity by complexes [Rh(**3**)(**6**)(cod)]BF_4, [Rh(**4**)(**6**)(cod)]BF_4, and [Rh(**5**)(**6**)-(cod)]BF_4, producing the *S* product in line with that observed previously for complex [Rh(**1**)(**6**)(cod)]BF_4.[39,55] Interestingly, the geometries of the ligands **3**–**5** are close to that of the urea-based ligand **1**, leading to a similar orientation of the hydrogen bond donor group involved in the hydrogen-bonding interactions. On the other hand, in ligand **2** the phosphine oxide group is directly connected to the phenyl substituent on the phosphine, inducing an important change in the geometry of the ligand (in comparison to ligand **1**). This difference in geometry of ligand **2** leads to a different orientation of the hydrogen bonds between the catalyst and the substrate. This difference in hydrogen bonding was already deduced from the NMR experiments and the DFT study performed on the precatalysts, and it translates to a lower selectivity in the hydrogenation of substrates **F** and **G** by the complex [Rh(**2**)(**6**)(cod)]BF_4. Therefore, the geometry of the ligand bearing the hydrogen bond acceptor has an important role in the structure of the supramolecular catalyst. Small differences in the structure of the catalyst can have important consequences on the outcome of the reaction, but interestingly the steric hindrance of the substituents on the different phosphine oxide groups (ligands **3**–**5**) does not influence the excellent selectivity observed for substrates **F** and **G**.

The reaction mechanism of the hydrogenation of substrate **G** by the complex [Rh(**3**)(**6**)(cod)]BF_4 was studied by means of NMR spectroscopy and DFT calculations (Figure 7). When a 0.02 M solution of complex [Rh(**3**)(**6**)(cod)]BF_4 in CD_2Cl_2 was hydrogenated at −80 °C for 1 h, the signals in the ^{31}P NMR spectrum completely disappeared and only traces of the precatalyst and traces of the hydrolyzed ligand could be detected. The broad signals observed in the ^{31}P NMR spectrum are attributed to the formation of undefined monomeric solvate species in solution, as previously observed in our experiments performed with the complex [Rh(**1**)(**6**)-(cod)]BF_4.[39]

Upon addition of 5 equiv of substrate **G**, new sets of doublets of doublets arise in the ^{31}P NMR spectrum. The new

DOI: 10.1021/acs.organomet.9b00484
Organometallics 2019, 38, 3961–3969

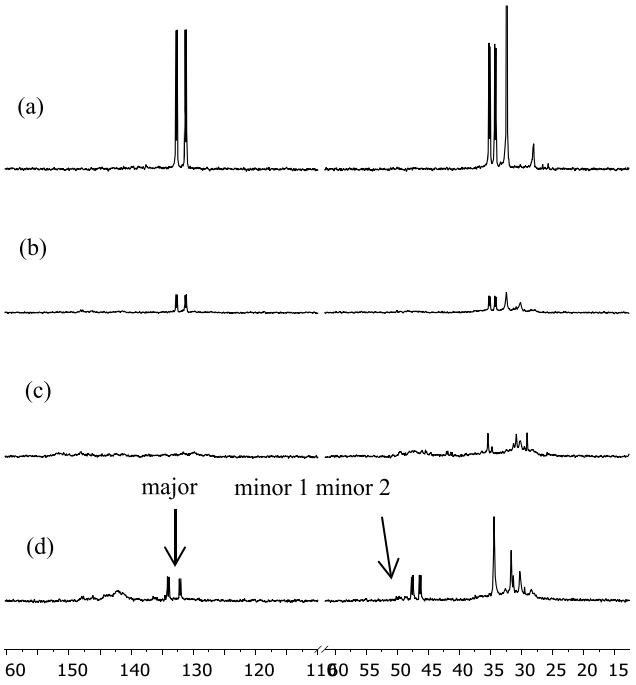

Figure 7. ^{31}P NMR spectra (162 MHz, CD_2Cl_2) of a sample initially containing a solution of [Rh(**3**)(**6**)(cod)]BF_4: (a) starting spectrum, 298 K; (b) hydrogenation under 5 bar at 193 K for 1 h (the sample was degassed and the spectrum was taken at 298 K); (c) the same sample with an additional hydrogenation for 30 min at 193 K (the sample was degassed and the spectrum was taken at 298 K); (d) spectrum after the addition of 5 equiv of substrate **G** at 298 K.

species observed in the ^{31}P NMR spectrum consist of a major species and two other minor species in the ratio major/minor1/minor2 of 4/1/1. Due to overlay of the signals of the minor species, coupling constants and chemical shifts could be established only for the major species ($\delta(P^1)$ dd, 133.09 ppm, $^1J_{P,Rh}$ = 307.6 Hz, $^2J_{P,P'}$ = 38.9 Hz; $\delta(P^2)$ dd, 46.96 ppm, $^1J_{P,Rh}$ = 205.6 Hz, $^2J_{P,P'}$ = 38.9 Hz). On the basis of our previous studies, these signals indicate the formation of substrate–chelate complexes. Also, integration of the signals allowed us to assign the singlet at δ 34.45 ppm to the PO group belonging to the major species observed in the ^{31}P NMR spectrum.

This hardly shifted signal of the PO group means that the PO group is not coordinated to the metal center but still is involved in hydrogen bond formation. The difference in chemical shifts between the PO of the precatalyst and the PO group in the major species ($\Delta\delta$ = 2.04 ppm with respect to the PO group in the precatalyst) indicates that the coordination of the substrate influences the orientation of the PO group. Due to the numerous signals in the ^{31}P and ^{13}C NMR spectra, no information could be obtained on the coordination mode of the substrate. To get more insight into the structure of the major chelate complex, we optimized the structures of the four possible diastereoisomers that can be formed upon coordination of the prochiral substrate to the complex (Figure 8). The most stable diastereoisomer (structure **A**, Figure 8) features two hydrogen bonds between the substrate and the catalyst. Indeed, the hydroxyl group of the substrate has a hydrogen bond interaction with the NH group of the phosphoramidite ligand and with the oxygen of the phosphine oxide group. Effectively, the hydroxyl group of the substrate is inserted in the PNH–PO hydrogen bond between the two ligands,

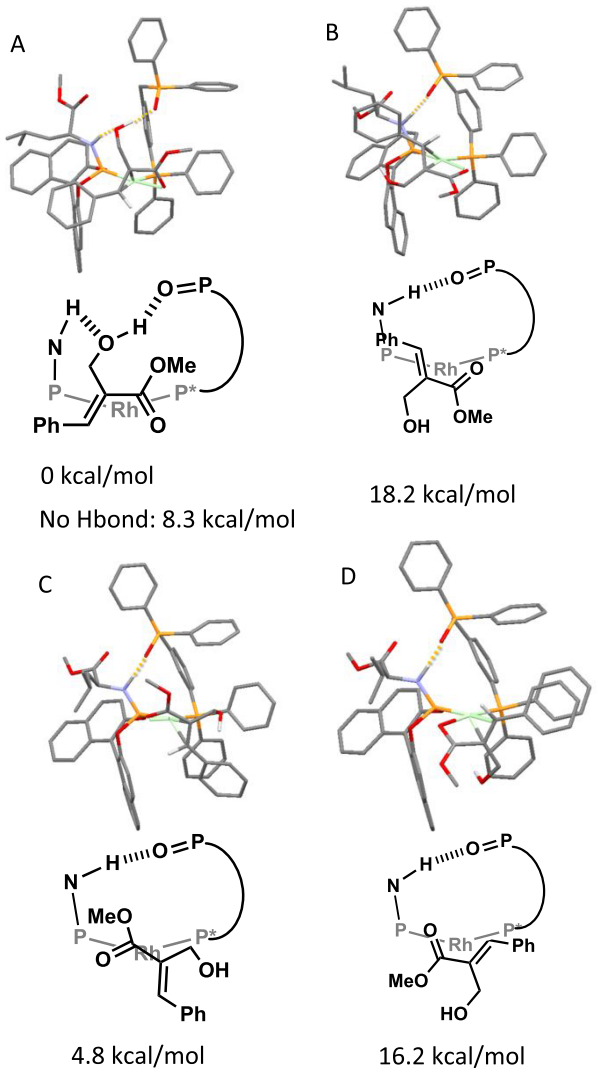

Figure 8. Calculated structures of the four possible catalyst–substrate complexes (optimized with DFT, def2-TZVP/disp3). Most of the hydrogen atoms have been removed for clarity (except from the hydrogen atoms involved in hydrogen bonds and the hydrogen atom on the hydroxyl group).

resulting in the stabilization of the catalyst–substrate complex. Also, we calculated the conformer of structure **A** in which the hydroxyl group is not interacting with the catalyst (with the hydroxyl group pointing away from the catalyst). Interestingly, this structure is 8.3 kcal mol^{-1} higher in energy than structure **A** (pro-*S* face) and also higher in energy than structure **C** (pro-*R* face). This large difference in energy as a result of hydrogen bond interactions between the catalyst and the substrate reflects the importance of the interaction, as the order of the stability of the possible catalyst–substrate adducts would change without H bonding.[54]

The catalyst–substrate complex was analyzed by 2D ^{1}H–^{1}H COSY NMR, revealing an upfield shift of the NH group of the phosphoramidite at δ 5.30 ppm. This chemical shift indicates that the NH group is still involved in a hydrogen bond in the catalyst–substrate complex. Also, the difference in chemical shift between the NH group in the catalyst–substrate complex and the NH group in the precatalyst ($\Delta\delta$ = 1.88 ppm) suggests an important modification of the geometry of the hydrogen bond between the two ligands. As can be seen in the calculated

DOI: 10.1021/acs.organomet.9b00484
Organometallics 2019, 38, 3961–3969

structure **A** (Figure 8), the NH group of the phosphoramidite forms a hydrogen bond with the OH group of the substrate, which is different from the hydrogen bond to the phosphine oxide found in the precomplex.

Detailed mechanistic studies on the urea-based system (complex [Rh(**1**)(**6**)(cod)]BF_4) showed how the hydrogen bond interaction between the substrate and the catalyst influences the rate and the selectivity.[55] To establish that the phosphine oxide analogue discussed in the current contribution operates via a similar mechanism, the activity of this catalyst was studied in more detail by kinetics and DFT calculations. The reaction progress was monitored under different conditions by gas uptake during the hydrogenation of substrate **G** (complexes [Rh(**1**)(**6**)(cod)]BF_4, [Rh(**2**)(**6**)-(cod)]BF_4, [Rh(**3**)(**6**)(cod)]BF_4, and [Rh(**5**)(**6**)(cod)]BF_4; Table 3). In comparison to the complex [Rh(**1**)(**6**)(cod)]BF_4 (first-generation catalyst), higher activities are observed with complexes [Rh(**3**)(**6**)(cod)]BF_4 and [Rh(**5**)(**6**)(cod)]BF_4, while excellent selectivity is retained (up to 99.7% ee). The TOF observed when complex [Rh(**2**)(**6**)(cod)]BF_4 was used is much lower. This complex has a different geometry, as is clear from the calculated structure, and this has an influence on the activity of the complex, underlining the importance of the orientation of the hydrogen bonding groups in the catalyst (entry 3, Table 3).

Table 3. Hydrogenation of Substrate G by Complexes [Rh(1)(6)(cod)]BF_4, [Rh(2)(6)(cod)]BF_4, [Rh(3)(6)(cod)]BF_4, and [Rh(5)(6)(cod)]BF_4[a]

complex	S/C ratio	conversn (%)[b]	TOF[c]	ee[d] (%)
Rh(**1**)(**6**)(cod)BF_4	1000	98	875	95.5
Rh(**3**)(**6**)(cod)BF_4	1000	100	3644	99.7
Rh(**2**)(**6**)(cod)BF_4	1000	39	335	96
Rh(**5**)(**6**)(cod)BF_4	1000	99	4561	99.2

[a]Reagents and conditions: [Rh] = 0.2 mM, S/C ratio = 1000, 25 °C, 20 h, $p(H_2)$ = 10 bar. [b]Determined by ^{1}H NMR. [c]Turnover frequencies calculated at 15% conversion. [d]Determined by HPLC.

In order to gain more insight into the mechanism of this new series of catalysts, we performed several kinetic experiments on the hydrogenation of substrate **G** by complex [Rh(**3**)(**6**)-(cod)]BF_4. Monitoring the reaction progress by gas uptake for experiments with different initial substrate concentrations reveals a positive order dependency of the reaction rate in the range 0.1 M-0.2 M on the substrate concentration. Also, experiments carried out at different pressures of hydrogen revealed a positive dependency of the TOF on the hydrogen concentration.

Complex [Rh(**1**)(**6**)(cod)]BF_4) was demonstrated previously to follow Michaelis–Menten (MM) kinetics in which the substrate reversibly associates to the catalyst before the rate-determining migration step. The kinetic data obtained for the hydrogenation of substrate **G** by the complex [Rh(**3**)(**6**)-(cod)]BF_4 also nicely fitted to the MM kinetic model (eq 1), providing the parameters given in Table 4.

$$V = \frac{V_{max}[S]}{K_{MM} + [S] + \frac{K_{MM}}{K_i}[P]} \quad (1)$$

The higher value of K_{MM} measured for complex [Rh(**3**)-(**6**)(cod)]BF_4 in comparison to [Rh(**1**)(**6**)(cod)]BF_4 suggests that binding of the substrate is weaker and that, under catalytic conditions, a larger fraction of the catalyst in solution is present as the solvate complex. This is in line with the NMR experiments, as only minor amounts of the catalyst–substrate complex were observed in solution in the presence of 5 equiv of substrate **G**. As the phosphine oxide (ligand **3**) is a stronger hydrogen bond acceptor then the urea function (ligand **1**), one may expect a stronger interaction with the substrate. However, these better hydrogen bond accepting properties also lead to a stronger interaction between the two ligands, and this hydrogen bond needs to be broken upon substrate binding, which requires more energy. As such, the use of a stronger hydrogen bond acceptor does not lead to a stronger association of the hydrogen-bonded substrate. Importantly, the complex [Rh(**3**)(**6**)(cod)]BF_4 has a higher maximum reaction rate in comparison to the urea catalyst complex [Rh(**1**)(**6**)(cod)]BF_4, suggesting that the stabilization by the hydrogen bond is stronger (Table 4). In order to confirm this, DFT calculations were performed.

Table 4. Michaelis–Menten Kinetic Parameters for the Asymmetric Hydrogenation of Substrate G by the Complexes [Rh(1)(6)(cod)]BF_4 and [Rh(3)(6)(cod)]BF_4

	[Rh(**1**)(**6**)(cod)]BF_4	[Rh(**3**)(**6**)(cod)]BF_4
V_{max} (M h^{-1})	0.38701	1.90494
K_{MM} (M)	0.04282	0.26012
K_i (M)	0.01449	0.02371

We studied the influence of the hydrogen bond interactions on the energy of the intermediates and the transition states involved in the mechanism of the reaction. Following our previous computational studies on the urea-based supramolecular system [Rh(**1**)(**6**)(cod)]BF_4, we calculated the energy profile of the hydrogenation of substrate **G** by the complex [Rh(**3**)(**6**)(cod)]BF_4. The similarities between the two supramolecular systems result in similarities in the mechanism. They both follow an unsaturated pathway in which the substrate coordinates to the catalyst prior to the oxidative addition of hydrogen. The calculated energy profiles of the complexes [Rh(**1**)(**6**)(cod)]BF_4 and [Rh(**3**)(**6**)(cod)]-BF_4 were plotted in the same graph to highlight the differences, taking the energy of the major diastereoisomer as a reference (Figure 9).

As can be seen from Figure 9, the pathway corresponding to complex [Rh(**3**)(**6**)(cod)]BF_4 (red path) has a lower overall energy barrier than the pathway provided by complex [Rh(**1**)(**6**)(cod)]BF_4 (blue line). The difference between the energy of the catalyst–substrate complex and the energy of the hydride migration transition state (Figure 10) is lowered by 2.25 kcal mol^{-1}. The decrease in the overall energy barrier is attributed to the enhanced strength of the hydrogen bond provided by the strong hydrogen bond donor properties of the phosphine oxide groups. Apparently, this hydrogen bond stabilization is stronger in the transition state (**D**) than in the substrate precomplex (**C**).

In order to evaluate the importance of the H-bond effect in the reaction mechanism of the catalyst [Rh(**3**)(**6**)(cod)]BF_4, we removed the hydrogen-bond interactions in structures **C** and **E** and the transition state **D** by replacing the hydroxyl group on the substrate by a hydrogen (Figure 11). The SCF energies of the structures were plotted on the same energy profile, taking the energy of the diasteromers as a reference. As can be seen in Figure 11, the hydrogen bond interaction is more pronounced at the step of hydride migration than at the

DOI: 10.1021/acs.organomet.9b00484
Organometallics 2019, 38, 3961–3969

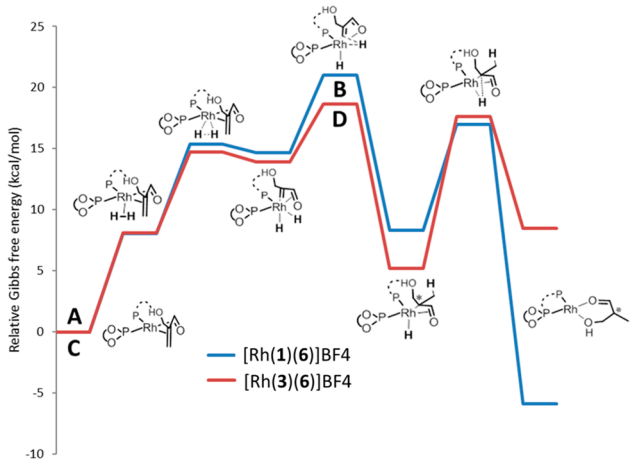

Figure 9. Energy profiles of the unsaturated pathways for the urea-based supramolecular catalyst [Rh(**1**)(**6**)(cod)]BF_4 (blue path) and the phosphine oxide-based supramolecular catalyst [Rh(**3**)(**6**)(cod)]-BF_4 (red path).

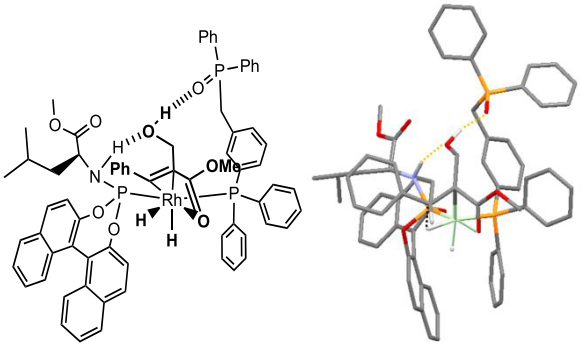

Figure 10. Optimized structure of the hydride migration transition state **D** ($\Delta G_{298\,K}$= +18.64 kcal mol^{-1}/**A**, $\upsilon^{\ddagger}$ = −616.9*i* cm^{-1}). All hydrogen atoms are omitted for clarity except the proton of the alkene and the hydrogen atoms involved in hydrogen bonds. Hydrogen bonds are drawn in orange. The black dotted line represents the hydride insertion to form the alkyl hydride species.

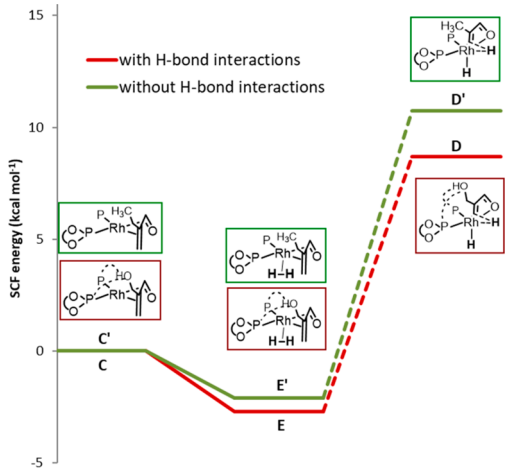

Figure 11. Relative SCF energies of the intermediates **C**, **E**, and **D** with and without hydrogen bond interactions between the catalyst and the substrate. **C** and **C′** are set to zero.

early steps. The intramolecular hydrogen bonds are responsible for the stabilization of the transition state **D** by approximately 2 kcal mol^{-1}, in comparison to the hydride migration step **D′** not featuring hydrogen bonds between the catalyst and the substrate. Most likely, the structure of the complex during the hydride migration step is favorable for hydrogen bond formation.

CONCLUSION

Through rational design, on the basis of mechanistic considerations, a second-generation catalyst based on supramolecular bidentate ligands was synthesized and evaluated in the rhodium-catalyzed asymmetric hydrogenation of several functionalized substrates. In this second generation of catalysts, supramolecular complexes [Rh(**3**)(**6**)(cod)]BF_4 and [Rh(**5**)-(**6**)(cod)]BF_4 are very efficient in the asymmetric hydrogenation of substrates **F** and **G**, both bearing a hydroxyl group, leading to almost perfect enantioselectivity (up to 99.9% ee). A mechanistic study demonstrates that two hydrogen bond interactions between the catalyst and the substrate are involved in the stabilization of a catalyst−substrate complex intermediate. Kinetic studies show that the reaction is faster when it is catalyzed by the phosphine oxide based catalysts Rh[(**3**)-(**6**)(cod)]BF_4 and [Rh(**5**)(**6**)(cod)]BF_4, suggesting hydrogen bond stabilization of the rate-determining transition state. Computational studies of the reaction mechanism of the hydrogenation reaction mediated by the complex [Rh(**3**)(**6**)-(cod)]BF_4 and comparison with the first-generation catalyst [Rh(**1**)(**6**)(cod)]BF_4 indeed reveal that the supramolecular interactions between the substrate and the catalyst in the complex [Rh(**3**)(**6**)(cod)]BF_4 stabilizes the transition state of the hydride migration step to a larger extent than for the substrate complex. This results in an overall lower energy barrier, and thus this catalyst displays a higher activity. The development of catalysts by rational approaches is based on longstanding established parameters such as steric effects, electronic effects, and bite angle effects. The flourishing number of supramolecular strategies implies that noncovalent interactions should also be taken into account in the design of a catalyst. This work highlights the potential of fine-tuning supramolecular interactions as a new tool to improve catalyst performance.

EXPERIMENTAL SECTION

Representative Procedures for the Synthesis of Ligands. *Synthesis of (3-Iodobenzyl)diphenylphosphine Oxide (**3-int**).* To a suspension of NaH (60% in mineral oil) (179 mg, 4.5 mmol) in freshly distilled THF (35 mL) at 0 °C was added diphenylphosphine oxide (606 mg, 3 mmol) under nitrogen. The mixture was stirred for 10 min. 3-Iodobenzyl bromide (3.3 mmol) was then added, and the mixture was stirred at room temperature for 6 h. Water was added (10 mL) to quench the reaction, the organic layer was extracted with ethyl acetate (40 mL) three times and dried over Na_2SO_4, and the volatile materials were removed under reduced pressure. The crude product was purified by flash chromatography on silica gel (ethyl acetate/dichloromethane, 2/8) to give the product as a white solid. The yield was 58%.

*Synthesis of (3-(Diphenylphosphanyl)benzyl)diphenylphosphine Oxide (**3**).* (3-Iodobenzyl)diphenylphosphine oxide (1.75 mmol, 730 mg), diphenylphosphine (317 μL, 1.82 mmol), trimethylamine (485 μL), and palladium(II) acetate (2 mg) were dissolved in acetonitrile (25 mL) under nitrogen, brought to reflux, and continued to reflux overnight. The next day, volatiles were evaporated under reduced pressure, and to the residue were added dry dichloromethane (30 mL) and degassed water (15 mL). The water phase was washed with dichloromethane, the combined organic layers were dried over Na_2SO_4 and filtered, and the solvent was removed under vacuum. The

DOI: 10.1021/acs.organomet.9b00484
Organometallics 2019, 38, 3961−3969

crude product was purified by flash chromatography on silica gel (100% ethyl acetate) to give the product as a white solid. The yield was 85%.

Representative Procedure for the Synthesis of Complexes: Synthesis of [Rh(3)(6)(cod)]BF_4. Ligand **3** (0.025 mmol, 1 equiv) and ligand **6** (0.025 mmol, 1 equiv) were placed in a dry-flamed Schlenk flask under an argon atmosphere. CD_2Cl_2 (0.3 mL) was dropped on them, leading to a transparent solution. The commercially available $[Rh(cod)_2]BF_4$ salt (0.025 mmol, 1 equiv) was placed in another flame-dried Schlenk flask under an argon atmosphere and was dissolved with 0.25 mL of CD_2Cl_2. The solution of the metal salt was added dropwise to the solution of ligands, and the medium was stirred for 30 min at room temperature. The solution was transferred to an NMR tube under an argon atmosphere.

Representative Procedure for the Catalysis Experiments. The hydrogenation experiments were carried out in a stainless steel autoclave (150 or 250 mL) charged with an insert suitable for 8 or 15 reaction vessels (including Teflon mini stirring bars) for conducting parallel reactions. The reaction vessels were prepared in a glovebox under an N_2 atmosphere. Except where noted, in a typical experiment, the reaction vessels were charged with 200 μL of a 1 mM solution of catalyst and 0.1 mmol of substrate in 0.8 mL of CH_2Cl_2. Before the catalytic reactions were started, the charged autoclave was purged three times with 5 bar of dihydrogen and then pressurized at 5−40 bar of H_2. The reaction mixtures were stirred at 25 °C for 16 h. After catalysis the pressure was released,the conversion was determined by ^{1}H NMR, and the enantiomeric purity was determined by chiral GC or HPLC.

■ ASSOCIATED CONTENT

Supporting Information

The Supporting Information is available free of charge on the ACS Publications Web site at DOI: xxx The Supporting Information is available free of charge on the ACS Publications website at DOI: 10.1021/acs.organomet.9b00484.

General considerations, details of syntheses, catalysis, kinetics, influence of the substrate concentration, influence of the temperature, and DFT calculations (PDF)

Cartesian coordinates for the calculated structures (XYZ)

■ AUTHOR INFORMATION

Corresponding Author

*E-mail for J.N.H.R.: j.n.h.reek@uva.nl.

ORCID

Bas de Bruin: 0000-0002-3482-7669

Joost N. H. Reek: 0000-0001-5024-508X

Notes

The authors declare no competing financial interest.

■ ACKNOWLEDGMENTS

Support for this work was generously provided by NWO, the dutch national science foundation. The work is part of the research priority sustainable chemistry from the University of Amsterdam.

■ REFERENCES

(1) Van Leeuwen, P. W. N. M. *Homogeneous Catalysis—understanding the Art*; Kluwer: Dordrecht, The Netherlands, 2004.

(2) Cornils, B.; Herrmann, W. A. Concepts in Homogeneous Catalysis : The Industrial View. *J. Catal.* **2003**, *216*, 23−31.

(3) Johnson, N. B.; Lennon, I. C.; Moran, P. H.; Ramsden, J. A. Industrial-Scale Synthesis and Applications of Asymmetric Hydrogenation Catalysts. *Acc. Chem. Res.* **2007**, *40* (12), 1291−1299.

(4) Tang, W.; Zhang, X. New Chiral Phosphorus Ligands for Enantioselective Hydrogenation. *Chem. Rev.* **2003**, *103* (8), 3029−3070.

(5) Jäkel, C.; Paciello, R. High-Throughput and Parallel Screening Methods in Asymmetric Hydrogenation. *Chem. Rev.* **2006**, *106* (7), 2912−2942.

(6) Chiba, M.; Takahashi, H.; Takahashi, H.; Morimoto, T.; Achiwa, K. Synthesis and Application of a Novel Bisphosphine Ligand, (−)-DIOCP, as an Unsymmetrized Diop to Prove the General Utility of New Designing Concept. *Tetrahedron Lett.* **1987**, *28* (32), 3675−3678.

(7) Takahashi, H.; Morimoto, T.; Achiwa, K. Highly Effective Catalytic Asymmetric Hydrogenations of α-Keto Esters and an α-Keto Acetal with New Neutral Chiral Pyrrolidinebisphosphine-Rhodium Complexes. *Chem. Lett.* **1987**, *16* (5), 855−858.

(8) Togni, A.; Breutel, C.; Schnyder, A.; Spindler, F.; Landert, H.; Tijani, A. A Novel Easily Accessible Chiral Ferrocenyldiphosphine for Highly Enantioselective Hydrogenation, Allylic Alkylation, and Hydroboration Reactions. *J. Am. Chem. Soc.* **1994**, *116* (9), 4062−4066.

(9) Holz, J.; Heller, D.; Stürmer, R.; Börner, A. Synthesis of the First Water-Soluble Chiral Tetrahydroxy Diphosphine Rh(I) Catalyst for Enantioselective Hydrogenation. *Tetrahedron Lett.* **1999**, *40* (39), 7059−7062.

(10) Yoon, T. P.; Jacobsen, E. N. Privileged Chiral Catalysts. *Science* **2003**, *299* (5613), 1691−1693.

(11) Imamoto, T.; Tamura, K.; Zhang, Z.; Horiuchi, Y.; Sugiya, M.; Yoshida, K.; Yanagisawa, A.; Gridnev, I. D. Rigid P-Chiral Phosphine Ligands with Tert-Butylmethylphosphino Groups for Rhodium-Catalyzed Asymmetric Hydrogenation of Functionalized Alkenes. *J. Am. Chem. Soc.* **2012**, *134*, 1754−1769.

(12) Teichert, J. F.; Feringa, B. L. Phosphoramidites : Privileged Ligands in Asymmetric Catalysis. *Angew. Chem., Int. Ed.* **2010**, *49*, 2486−2528.

(13) Reetz, M. T.; Sell, T.; Meiswinkel, A.; Mehler, G. A New Principle in Combinatorial Asymmetric Transition-Metal Catalysis: Mixtures of Chiral Monodentate P Ligands. *Angew. Chem., Int. Ed.* **2003**, *42* (7), 790−793.

(14) Reetz, M. T.; Mehler, G. Mixtures of Chiral and Achiral Monodentate Ligands in Asymmetric Rh-Catalyzed Olefin Hydrogenation: Reversal of Enantioselectivity. *Tetrahedron Lett.* **2003**, *44* (24), 4593−4596.

(15) Reetz, M. T.; Bondarev, O. Mixtures of Chiral Phosphorous acid Diesters and Achiral P Ligands in the Enantio- and Diastereoselective Hydrogenation of Ketimines. *Angew. Chem., Int. Ed.* **2007**, *46* (24), 4523−4526.

(16) Reetz, M. T.; Guo, H. Mixtures of Monodentate P-Ligands as a Means to Control the Diastereoselectivity in Rh-Catalyzed Hydrogenation of Chiral Alkenes. *Beilstein J. Org. Chem.* **2005**, *1*, 2−7.

(17) Reetz, M. T.; Fu, Y.; Meiswinkel, A. Nonlinear Effects in Rh-Catalyzed Asymmetric Olefin Hydrogenation Using Mixtures of Chiral Monodentate P Ligands. *Angew. Chem., Int. Ed.* **2006**, *45* (9), 1412−1415.

(18) van den Berg, M.; Minnaard, A. J.; Schudde, E. P.; van Esch, J.; de Vries, A. H. M.; de Vries, J. G.; Feringa, B. L. Highly Enantioselective Rhodium-Catalyzed Hydrogenation with Monodentate Ligands. *J. Am. Chem. Soc.* **2000**, *122* (46), 11539−11540.

(19) Peña, D.; Minnaard, A. J.; de Vries, J. G.; Feringa, B. L. Highly Enantioselective Rhodium-Catalyzed Hydrogenation of β-Dehydroamino Acid Derivatives Using Monodentate Phosphoramidites. *J. Am. Chem. Soc.* **2002**, *124* (49), 14552−14553.

(20) Hu, A.-G.; Fu, Y.; Xie, J.; Zhou, H.; Wang, L.-X.; Zhou, Q.-L. Monodentate Chiral Spiro Phosphoramidites: Efficient Ligands for Rhodium-Catalyzed Enantioselective Hydrogenation of Enamides. *Angew. Chem., Int. Ed.* **2002**, *41* (13), 2348−2350.

(21) Van Leeuwen, P. W. N. M.; Freixa, Z. Supramolecular Catalysis: Refocusing Catalysis. In *Supramolecular Catalysis*; Wiley-VCH: Weinheim, Germany, 2008; pp 255−299.

DOI: 10.1021/acs.organomet.9b00484
Organometallics 2019, 38, 3961−3969

(22) Breit, B.; Seiche, W. Hydrogen Bonding as a Construction Element for Bidentate Donor Ligands in Homogeneous Catalysis : Regioselective Hydroformylation of Terminal Alkenes. *J. Am. Chem. Soc.* **2003**, *125*, 6608−6609.
(23) Breit, B. Supramolecular Approaches to Generate Libraries of Chelating Bidentate Ligands for Homogeneous Catalysis. *Angew. Chem., Int. Ed.* **2005**, *44* (42), 6816−6825.
(24) Weis, M.; Waloch, C.; Seiche, W.; Breit, B. Self-Assembly of Bidentate Ligands for Combinatorial Homogeneous Catalysis: Asymmetric Rhodium-Catalyzed Hydrogenation. *J. Am. Chem. Soc.* **2006**, *128* (13), 4188−4189.
(25) Birkholz, M.-N.; Dubrovina, N. V.; Jiao, H.; Michalik, D.; Holz, J.; Paciello, R.; Breit, B.; Börner, A. Enantioselective Hydrogenation with Self-Assembling Rhodium Phosphane Catalysts: Influence of Ligand Structure and Solvent. *Chem. - Eur. J.* **2007**, *13* (20), 5896−5907.
(26) Duckmanton, P. A.; Blake, A. J.; Love, J. B.; Park, U. V.; Uni, V.; Ng, N. Palladium and Rhodium Ureaphosphine Complexes : Exploring Structural and Catalytic Consequences of Anion Binding. *Inorg. Chem.* **2005**, *44* (22), 7708−7710.
(27) Knight, L. K.; Freixa, Z.; van Leeuwen, P. W. N. M.; Reek, J. N. H. Supramolecular Trans -Coordinating Phosphine Ligands. *Organometallics* **2006**, *25* (4), 954−960.
(28) Sandee, A. J.; van der Burg, A. M.; Reek, J. N. H. UREAphos: Supramolecular Bidentate Ligands for Asymmetric Hydrogenation. *Chem. Commun.* **2007**, No. 8, 864−866.
(29) Gulyás, H.; Benet-Buchholz, J.; Escudero-Adan, E. C.; Freixa, Z.; van Leeuwen, P. W. N. M. Ionic Interaction as a Powerful Driving Force for the Formation of Heterobidentate Assembly Ligands. *Chem. - Eur. J.* **2007**, *13* (12), 3424−3430.
(30) Pignataro, L.; Lynikaite, B.; Cvengroš, J.; Marchini, M.; Piarulli, U.; Gennari, C. Combinations of Acidic and Basic Monodentate Binaphtholic Phosphites as Supramolecular Bidentate Ligands for Enantioselective Rh-Catalyzed Hydrogenations. *Eur. J. Org. Chem.* **2009**, *2009*, 2539−2547.
(31) Pignataro, L.; Lynikaite, B.; Colombo, R.; Carboni, S.; Krupička, M.; Piarulli, U.; Gennari, C. Combination of a Binaphthol-Derived Phosphite and a C1-Symmetric Phosphinamine Generates Heteroleptic Catalysts in Rh- and Pd-Mediated Reactions. *Chem. Commun.* **2009**, 3539.
(32) Slagt, V. F.; Reek, J. N. H.; Kamer, P. C. J.; van Leeuwen, P. W. N. M. Assembly of Encapsulated Transition Metal Catalysts. *Angew. Chem., Int. Ed.* **2001**, *40*, 4271−4274.
(33) Slagt, V. F.; van Leeuwen, P. W. N. M.; Reek, J. N. H. Bidentate Ligands Formed by Self-Assembly. *Chem. Commun.* **2003**, 2474−2475.
(34) Slagt, V. F.; Kamer, P. C. J.; van Leeuwen, P. W. N. M.; Reek, J. N. H. Encapsulation of Transition Metal Catalysts by Ligand-Template Directed Assembly. *J. Am. Chem. Soc.* **2004**, *126*, 1526−1536.
(35) Jiang, X.-B.; Lefort, L.; Goudriaan, P. E.; de Vries, A. H. M.; van Leeuwen, P. W. N. M.; de Vries, J. G.; Reek, J. N. H. Screening of a Supramolecular Catalyst Library in the Search for Selective Catalysts for the Asymmetric Hydrogenation of a Difficult Enamide Substrate. *Angew. Chem., Int. Ed.* **2006**, *45* (8), 1223−1227.
(36) Jiang, X.-B.; van Leeuwen, P. W. N. M.; Reek, J. N. H. SUPRAphos-Based Palladium Catalysts for the Kinetic Resolution of Racemic Cyclohexenyl Acetate. *Chem. Commun.* **2007**, 2287−2289.
(37) Goudriaan, P. E.; Kuil, M.; Jiang, X.-B.; van Leeuwen, P. W. N. M.; Reek, J. N. H. SUPRAPhos Ligands for the Regioselective Rhodium Catalyzed Hydroformylation of Styrene Forming the Linear Aldehyde. *Dalton. Trans.* **2009**, 1801−1805.
(38) Breuil, P.-A. R.; Patureau, F. W.; Reek, J. N. H. Singly Hydrogen Bonded Supramolecular Ligands for Highly Selective Rhodium-Catalyzed Hydrogenation Reactions. *Angew. Chem., Int. Ed.* **2009**, *48* (12), 2162−2165.
(39) Daubignard, J.; Detz, R. J.; Jans, A. C. H.; de Bruin, B.; Reek, J. N. H. Rational Optimization of Supramolecular Catalysts for the Rhodium-Catalyzed Asymmetric Hydrogenation Reaction. *Angew. Chem., Int. Ed.* **2017**, *56* (42), 13056−13060.
(40) Grushin, V. V. Mixed Phosphine − Phosphine Oxide Ligands. *Chem. Rev.* **2004**, *104*, 1629−1662.
(41) Baker, M. J. PROCESS FOR THE CARBONYLATION OF METHANOL OR A REACTIVE DERVATIVE THEREOF, US Patent appl. 5488153, 1996.
(42) Carrow, B. P.; Nozaki, K. Synthesis of Functional Polyolefins Using Cationic Bisphosphine Monoxide−Palladium Complexes. *J. Am. Chem. Soc.* **2012**, *134* (21), 8802−8805.
(43) Etter, M. C.; Baures, P. W. Triphenylphosphine Oxide as a Crystallization Aid. *J. Am. Chem. Soc.* **1988**, *110*, 639−640.
(44) Kryschenko, Y. K.; Seidel, S. R.; Arif, A. M.; Stang, P. J. Coordination-Driven Self-Assembly of Predesigned Supramolecular Triangles. *J. Am. Chem. Soc.* **2003**, *125* (17), 5193−5198.
(45) Trujillo, C.; Sánchez-sanz, G.; Alkorta, I.; Elguero, J. Thermodynamic and Hydrogen-Bond Basicity of Phosphine Oxides : Effect of the Ring Strain. *Comput. Theor. Chem.* **2012**, *994*, 81−90.
(46) Oh, S. Y.; Nickels, C. W.; Garcia, F.; Jones, W.; Friščić, T. Switching between Halogen- and Hydrogen-Bonding in Stoichiometric Variations of a Cocrystal of a Phosphine Oxide. *CrystEngComm* **2012**, *14* (19), 6110.
(47) Sun, H.; Hunter, C. A.; Navarro, C.; Turega, S. Relationship between Chemical Structure and Supramolecular Effective Molarity for Formation of Intramolecular H-Bonds. *J. Am. Chem. Soc.* **2013**, *135* (35), 13129−13141.
(48) Ligands **1**, **2**, **6**, and **7** were synthesized according to existing literature procedures.
(49) Blagborough, T. C.; Davis, R.; Ivison, P. Some Transition Metal Complexes of Ph2P(CH2)NP(O)Ph2 (n = 1, 2) and Ph2P(CH2)P(S)Ph2. *J. Organomet. Chem.* **1994**, *467* (1), 85−94.
(50) In this system, the chemical shift of the PNH group in the system Rh(triphenylphosphine)(**6**) was taken as a reference in the assignment of the strength of the interaction.
(51) Steiner, T. The Hydrogen Bond in the Solid State. *Angew. Chem., Int. Ed.* **2002**, *41* (1), 48−76.
(52) The stability of the H-bonded complexes might be overestimated, as the free energy of the structures was obtained by gas-phase geometry optimization without COSMO solvent corrections.
(53) See the Supporting Information.
(54) Upon hydrogenation of the substrate−catalyst complex **A** at low temperature, no other intermediates could be detected. After hydrogenation, the product of the catalysis is obtained with 96% ee in favor of the *S* enantiomer.
(55) Daubignard, J.; Lutz, M.; Detz, R. J.; de Bruin, B.; Reek, J. N. H. Origin of the Selectivity and Activity in the Rhodium-Catalyzed Asymmetric Hydrogenation Using Supramolecular Ligands. *ACS Catal.* **2019**, *9*, 7535.

DOI: 10.1021/acs.organomet.9b00484
Organometallics 2019, 38, 3961−3969